nature geoscience

LETTERS

PUBLISHED ONLINE: 21 MARCH 2010 | DOI: 10.1038/NGEO817

Heterogeneous nucleation of ice particles on glassy aerosols under cirrus conditions

Benjamin J. Murray[1]*, Theodore W. Wilson[1], Steven Dobbie[2], Zhiqiang Cui[2], Sardar M. R. K. Al-Jumur[2], Ottmar Möhler[3], Martin Schnaiter[3], Robert Wagner[3], Stefan Benz[3], Monika Niemand[3], Harald Saathoff[3], Volker Ebert[4,5], Steven Wagner[4] and Bernd Kärcher[6]

Ice clouds in the tropical tropopause layer play a key role in dehydrating air as it enters the stratosphere[1,2]. However, *in situ* measurements show that water vapour within these clouds is unexpectedly supersaturated[3–5]; normally the growth of ice crystals rapidly quenches supersaturation[3]. The high in-cloud humidity may be related to the low number of ice crystals found in these clouds[4,6], but low ice number densities are inconsistent with standard models of cirrus cloud formation involving homogeneous freezing of liquid aerosols[7]. Aqueous aerosols rich in organic matter are ubiquitous in the atmosphere[8,9], and under cirrus conditions they are known to become glassy[10,11], that is, amorphous, non-crystalline solids. Here we report experiments in a cloud simulation chamber that demonstrate heterogeneous nucleation of ice on glassy solution droplets. Cirrus residues measured *in situ* showed ice nuclei rich in oxidized organic matter[12], consistent with heterogeneous nucleation on glassy aerosols. In addition, using a one-dimensional cirrus model, we show that nucleation on glassy aerosols may explain low ice crystal numbers and high in-cloud humidity in the tropical tropopause layer. We propose that heterogeneous nucleation on glassy aerosols is an important mechanism for ice nucleation in the tropical tropopause layer.

It was recently shown that aqueous solution droplets containing a range of soluble oxygenated organic compounds can become glassy under upper tropospheric conditions[10,11]. Glassy solids have an amorphous (non-crystalline) structure in which the diffusion of molecules is negligibly small. The glass-transition temperature (T_g) is the temperature below which the viscosity of a liquid reaches such extreme values that it becomes a solid (an atmospheric glassy aerosol particle is analogous to a child's toy marble). Low-volatility organic compounds are known to be ubiquitous in atmospheric aerosols; in fact, single-particle mass spectrometry shows that background aerosols in the tropical tropopause layer (TTL, ~12–18 km, ~180–200 K) contain approximately 30–70% by mass organic material[8]. Hence, it was suggested that many TTL aerosol particles are aqueous glassy solids[10,11]. However, the role of glassy particles in cloud formation was only a matter of speculation[10,11].

To test the impact of glassy aerosols on cold ice cloud formation, for the first time, we carried out a sequence of experiments at the Aerosol Interactions and Dynamics in the Atmosphere (AIDA) cloud simulation chamber. The AIDA chamber is an 84 m^3 highly instrumented vessel that can be cooled to 183 K. To simulate cloud formation, particles were introduced to the chamber to form an aerosol and the pressure was reduced by pumping. This expansion caused the remaining air in the chamber to cool adiabatically and the relative humidity therefore increased.

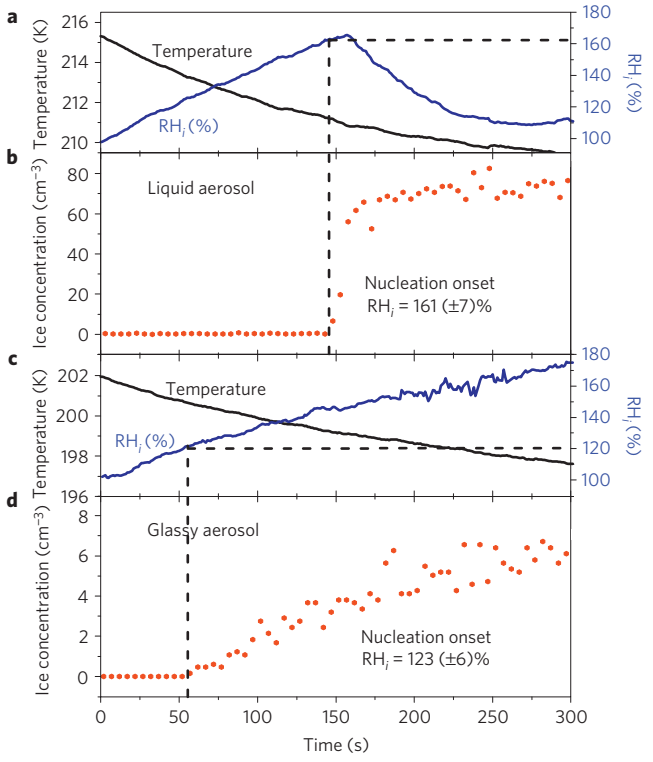

Figure 1 | Ice particle concentrations for expansion chamber experiments. **a**–**d**, The temperature and relative humidity (using *in situ* laser absorption spectroscopy at 1.37 μm; ref. 15) in the chamber (**a**,**c**) and the ice particle concentrations determined by an optical particle counter (**b**,**d**) during experiments starting with liquid (**a**,**b**) and glassy (**c**,**d**) citric acid aerosol particles. The points at which ice particles were first observed to form using laser depolarization are also indicated by dashed vertical lines.

The chamber has been used in the past to test the water-activity-based parameterization[13] for nucleation in solution droplets free

[1]School of Chemistry, University of Leeds, Woodhouse Lane, Leeds LS2 9JT, UK, [2]School of Earth and Environment, University of Leeds, Woodhouse Lane, Leeds LS2 9JT, UK, [3]Institute for Meteorology and Climate Research, Karlsruhe Institute of Technology, Postfach 3640, 76021, Germany, [4]Institute of Physical Chemistry, University of Heidelberg, Im Neuenheimer Feld 253, D-69120 Heidelberg, Germany, [5]Physikalisch-Technische Bundesanstalt, Bundesallee 100, D-38116 Braunschweig, Germany, [6]Deutsches Zentrum für Luft- und Raumfahrt, Institut für Physik der Atmosphäre, Oberpfaffenhofen, D-82234 Wessling, Germany. *e-mail: B.J.Murray@Leeds.ac.uk.

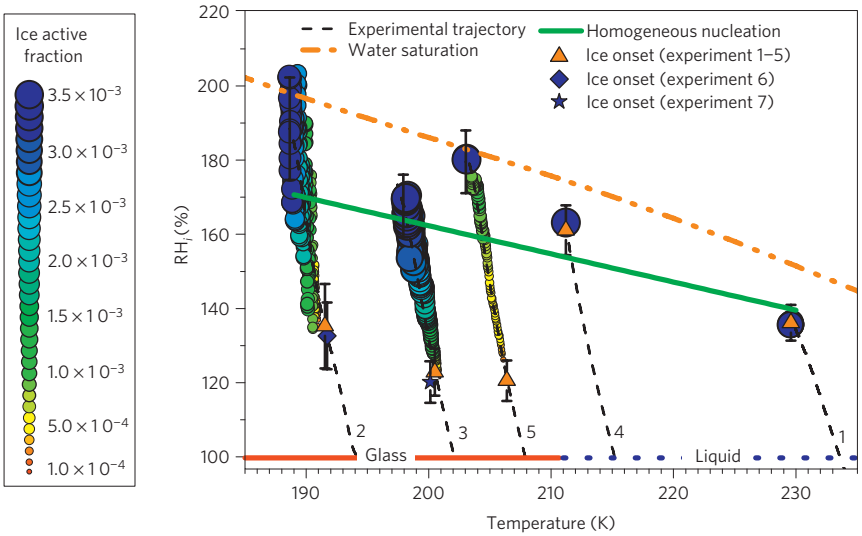

Figure 2 | The onset of ice formation and fraction of citric acid aerosol particles that nucleated ice in a number of expansion experiments. Runs 1 and 4 were with liquid aerosol, whereas runs 2, 3 and 5 were with glassy aerosol. For these expansion experiments, idealized (T–RH_i) trajectories are shown. Conditions at which ice was first observed to form using laser depolarization measurements are shown. The size of the circles indicates the fraction of aerosol particles that activated to ice (f_{ice}) determined using an optical particle counter. The error bars indicate the uncertainty in the measurement of RH_i. See Supplementary Information for further discussion of this figure.

of any solid impurities (homogeneous nucleation; ref. 14) as well as in studies to quantify how efficiently solid particles catalyse ice formation (heterogeneous ice nucleation; ref. 15). Here, we used the same expansion technique, but we began our experiments with citric acid particles that were either in a glassy solid state below 212 K or a liquid state above 212 K (see Supplementary Information for discussions of the atmospheric relevance of citric acid and for the 212 K threshold). Laser depolarization measurements showed that the aqueous citric acid aerosol particles did not effloresce in the AIDA chamber.

The number density of ice crystals (N_{ice} cm^{-3}) that nucleated during two expansion experiments with a suspension of citric acid particles is shown in Fig. 1 together with the corresponding temperature and relative humidity with respect to hexagonal ice (RH_i) measurements. The results from the experiment in which we started with a liquid (non-glassy) aerosol at 215 K are shown in Fig. 1a,b. As the temperature fell the RH_i within the chamber increased and when it reached a value of 161 (±7)% ice particles were observed to start forming. N_{ice} rapidly increased to ~70 cm^{-3} before the growth of these crystals quenched the supersaturation preventing further nucleation. This is the expected behaviour for liquid aerosol particles in which ice nucleated homogeneously[14,16].

Figure 1c,d shows results from a second expansion experiment where the initial temperature was 202 K and the aerosol particles were therefore glassy solids. This experiment was carried out in a very similar way (cooling rates ~10^2 K h^{-1}) to the previous one, but ice nucleation started at an RH_i of only 123 (±6)%, whereas homogeneous nucleation would be expected at ~164%. Furthermore, and vitally important in terms of cirrus formation, far fewer ice crystals nucleated. Even at 170% RH_i only ~6 cm^{-3} ice particles had nucleated, as opposed to ~70 cm^{-3} in the experiment starting with liquid particles. The initial number and size of aerosol particles in both experiments was similar (~10^3 cm^{-3}; mode diameter ~150 nm) and cannot explain these substantial differences.

We repeated expansion experiments for a range of temperatures and the results are summarized in Fig. 2. In the experiments starting with liquid citric acid solution droplets (experiments 1 and 4), nucleation occurred close to the values expected for homogeneous nucleation within aqueous solution droplets (solid green line). In the experiments starting with a glassy aerosol (2, 3 and 5), ice first nucleated at least 30% below the RH_i at which homogeneous nucleation would be expected in liquid droplets. In all cases where we started with a glassy aerosol, we observed a slow increase in the fraction of aerosol particles that activated to ice (f_{ice}) after the initial nucleation event. These results show, for the first time, that the glassy aerosol particles nucleated ice heterogeneously over a range of RH_i. In addition, it seems that the heterogeneous effect is less strong when close to the glass transition. The order in which these experiments were done is indicated in Fig. 2 (runs 1–5); we went from the liquid regime, to the glassy regime, back to the liquid regime and finally back into the glassy regime with the same aerosol. This shows that the glass transition is fully reversible and heterogeneous ice nucleation is a property of the glassy aerosol particles and not of the contaminating particles or crystalline citric acid. This suggests that a small shift in temperature can result in very different nucleation behaviour and, as we will show later, very different cloud properties. The physical mechanism with which glassy particles induce ice formation is not known and deserves further study.

Our finding that glassy aerosol particles nucleate ice heterogeneously at low RH_i is consistent with recent *in situ* measurements that showed TTL ice particles formed overwhelmingly from particles rich in oxidized organic material[12]. This is striking because in studies of other cloud types, organic particles were preferentially excluded from the ice phase[17]. We suggest that the organic-rich particles found within TTL ice particles were in fact glassy aqueous solution droplets that served as heterogeneous nuclei.

It is well known that heterogeneous nucleation can substantially alter the properties of cirrus clouds[18]. Here we illustrate the impact of heterogeneous nucleation of ice by glassy aerosols on TTL cirrus using a one-dimensional column model. This model is described elsewhere[19] and pertinent details are given in the Methods section and Supplementary Information.

As a control experiment, we first ran the model with only homogeneous nucleation in liquid aerosol particles allowed (HOM). These runs were compared with others where we allowed heterogeneous nucleation on glassy aerosol particles with an efficiency based on the chamber data (HET). In our HET runs,

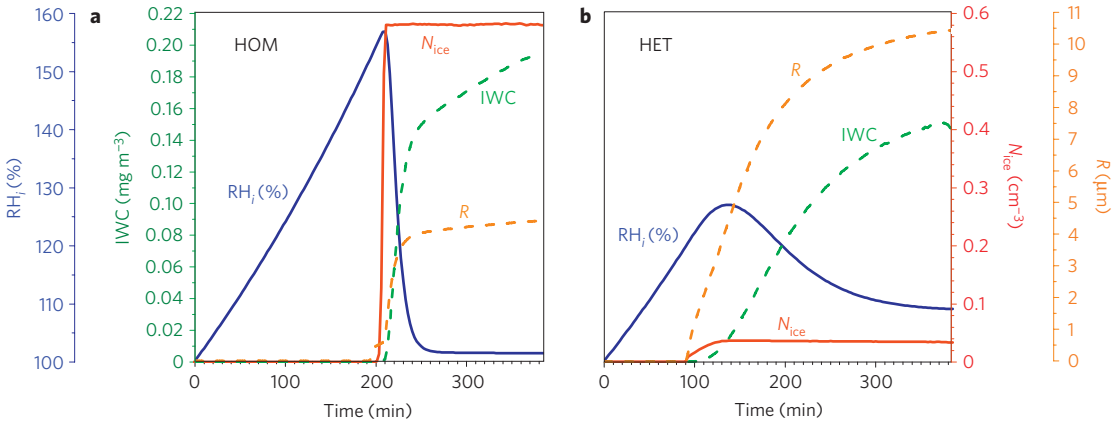

Figure 3 | Time series of model results averaged between 17.25 and 17.35 km. a, The results for a run in which only homogeneous nucleation in liquid aerosol particles was allowed. **b**, The results of a run in which 50% of the aerosol particles were assumed to be glassy and a fraction, defined by the experiments (see the Methods section), of these were allowed to nucleate ice heterogeneously. The cooling rate in these model runs was 0.76 K h^{-1}, equivalent to an updraft of 3 cm s^{-1}.

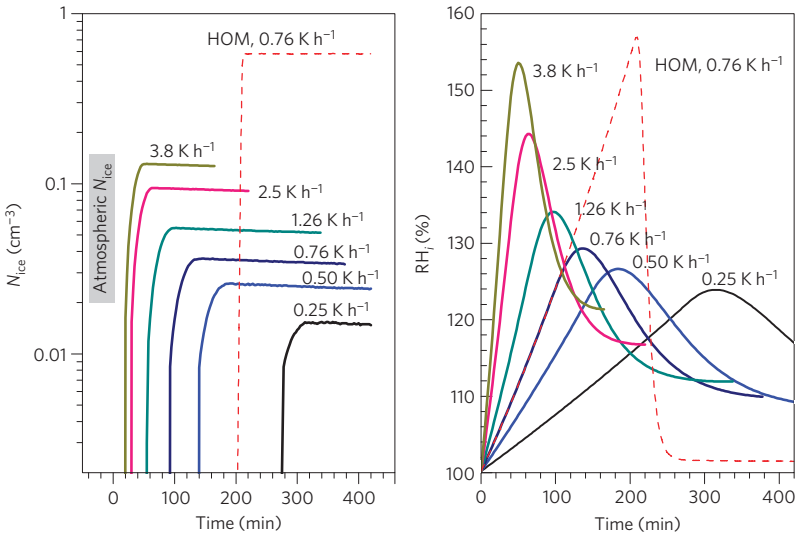

Figure 4 | Model result for N_{ice} and RH_i allowing heterogeneous nucleation on glassy particles, for a range of cooling rates. Other conditions were the same as in Fig. 3. Model runs are truncated when the cloud sedimented out of the 17.25–17.35 km layer. It is shown that more ice crystals nucleate for larger updrafts. This leads to more rapid relaxation of RH_i towards the quasi-steady state, but the competition between cooling and growth of ice crystals is such that the steady state remains higher. See Supplementary Information for associated IWC and *R*, as well as for model runs with different conditions. The solid grey bar indicates the range of N_{ice} observed in the TTL (ref. 7).

we split 100 cm^{-3} aerosol particles evenly into liquid and glassy populations (that is, $N_{glass} = 50$ cm^{-3}) and used the measured $f_{ice}(RH_i)$ to describe heterogeneous nucleation (see the Methods section). This is compared with a situation where all 100 cm^{-3} aerosol particles were liquid in the HOM runs.

Figure 3 summarizes the RH_i, mean radius (*R*), ice water content (IWC) and N_{ice} averaged between 17.25 and 17.35 km as a function of time for both HOM and HET runs. Cloud formation was forced by a cooling rate of 0.76 K h^{-1} in this case (equivalent updraft rate = 3 cm s^{-1}); this is consistent with cooling rates expected in the TTL (ref. 20).

In the HOM run (Fig. 3a), we can see that RH_i increases to a peak at ~160% where ice nucleated homogeneously in liquid droplets. The growth of the large number (0.58 cm^{-3}) of resulting ice crystals rapidly quenches the RH_i and within a few tens of minutes the cloud was close to equilibrium with the ambient humidity (that is, at ~100% RH_i).

In the HET run (Fig. 3b), the development of the cloud was very different to the HOM case. RH_i increased to a threshold of only ~120% before ice particles began to form and the RH_i peaked at 130%; thus, homogeneous nucleation in the liquid droplets did not occur. In this case only 0.035 cm^{-3} (35 l^{-1}) ice particles nucleated; this is a factor of ~17 less ice crystals than nucleated in the HOM run. *In situ* measurements show that N_{ice} in TTL cirrus is typically <0.1 cm^{-1} (refs 4, 7, 21). Varying model cooling rates between 0.25 and 3.8 K h^{-1} (1–15 cm s^{-1}) leads to 0.015–0.13 cm^{-3} ice particles (see Fig. 4). The low values of N_{ice} produced by heterogeneous nucleation on glassy aerosols are consistent with measurements in the TTL.

The small numbers of ice crystals grow ~2.3 times larger in the HET case compared with the HOM case. This substantially alters the final cloud properties, with an optical depth of about 0.035 for the HOM case and 0.012 for HET (for a cooling rate of 0.76 K h^{-1}). The influence of the nucleation mechanism on the radiative properties of cirrus is therefore likely to be significant, and will be addressed in the future.

Heterogeneous nucleation on glassy aerosol particles also leads to persistent in-cloud humidity much greater than 100%. The

small numbers of ice crystals have a relatively small surface area available for uptake of water vapour and therefore relaxation of the supersaturation is inefficient. In the model run in Fig. 3 it takes over 1 h for RH_i to fall to 120% and 3.5 h to come to a quasi-steady state of ~110%; that is, never reaching saturation (100%). The quasi-steady RH_i of 110% is higher than in HOM because fewer ice crystals are present in HET, balancing the cooling. This is consistent with previous cloud modelling studies that included nucleation on some unspecified nuclei[4,22–24]. Mineral particles are too rare in the TTL to account for the observed N_{ice} (ref. 8), and in addition, their nucleation efficiency will most likely be reduced by coatings[15,25]. It has been suggested that low ice concentrations may be explained if the correct number of crystalline and uncoated ammonium sulphate particles nucleate ice at low supersaturation under TTL conditions[7]. Other potential mechanisms for high in-cloud humidity have been discussed[3] and should not be ruled out. For example, if TTL cirrus clouds were composed of cubic ice[26–28] we would expect the in-cloud vapour pressure to be even larger because the equilibrium vapour pressure of cubic ice is greater than that of hexagonal ice[5].

Further model runs showed that long relaxation times and in-cloud $RH_i > 100\%$ are produced with cooling rates between 0.25 (1 cm s^{-1}) and 3.8 K h^{-1} (15 cm s^{-1}) (Fig. 4). Only with cooling rates greater than 3.8 K h^{-1} was the RH_i driven to the homogeneous nucleation limit, in which case many ice crystals nucleated and the supersaturation was rapidly quenched. Model runs included in the Supplementary Information also show that low number densities and high in-cloud humidity are produced for a range of TTL temperatures and also when assuming only 10% of the aerosol particles are glassy rather than the 50% assumed for the runs shown in Figs 3 and 4.

In the past it was proposed that cloud formation would be suppressed if glassy aerosol particles dominated the aerosol population and this might provide an explanation for extreme out-of-cloud supersaturations[10]. We conclude here, on the basis of our modelling work, that extreme supersaturations should not occur where the atmosphere contains more than ~10 cm^{-3} glassy particles. Very high supersaturations were reached in the chamber experiments only because of the fast cooling rates used there.

This study highlights an important new nucleation mechanism for cirrus. We have shown that nucleation on glassy aerosol particles can explain the large in-cloud humidity and the low ice concentrations observed in the TTL. However, the role of glassy aerosols in cloud formation needs to be explored further to quantify their impact on climate and stratospheric chemistry. Research is needed to determine the fraction of aerosol particles in the TTL that are glassy and also how or whether human activities are influencing this fraction to investigate a potential glassy aerosol indirect effect.

Methods

In our study we used the Advanced Particle Simulation Code (APSC*m*-1D; ref. 19), a one-dimensional column model with explicit aerosol microphysics and Lagrangian tracking of ice crystals. Idealized temperature, pressure and RH_i profiles were used to initiate the model (see Supplementary Fig. S3); all values are within the range of aircraft measurements in the TTL region[6,29]. Ice formation in the model can occur either through homogeneous nucleation of solution droplets, which is described by the water-activity-based model[13], or through heterogeneous nucleation on glassy aerosol particles. The latter was defined in the model using a fit to the experimentally determined values of f_{ice} in run 3 (Fig. 2) and is described by the equation $f_{ice} = 7.7211 \times 10^{-5}\ RH_i(\%) - 9.2688 \times 10^{-3}$ for $RH_i = 121$–170% and $f_{ice} = 0$ for $RH_i < 121$. The number of ice crystals nucleated heterogeneously was defined by $f_{ice}N_{glass}$ (where N_{glass} is the number of glassy aerosol particles corrected for the number of ice particles already nucleated heterogeneously) at any one RH_i.

Vertical advection in the model is simulated by applying a uniform cooling across the whole layer at a defined rate. The mass accommodation coefficient of H_2O on ice is set at 0.5. For simplicity, a monomodal aerosol particle population of 100 cm^{-3} with 100 nm diameter is assumed. Water and ice equilibrium vapour pressures are taken from the literature[30].

Received 28 October 2009; accepted 8 February 2010; published online 21 March 2010

References

1. Holton, J. R. & Gettleman, A. Horizontal transport and the dehydration of the stratosphere. *Geophys. Res. Lett.* **28,** 2799–2802 (2001).
2. Jensen, E. J., Toon, O. B., Pfister, L. & Selkirk, H. B. Dehydration of the upper troposphere and lower stratosphere by subvisible cirrus clouds near the tropical tropopause. *Geophys. Res. Lett.* **23,** 825–828 (1996).
3. Peter, T. *et al.* When dry air is too humid. *Science* **314,** 1399–1402 (2006).
4. Krämer, M. *et al.* Ice supersaturations and cirrus cloud crystal numbers. *Atmos. Chem. Phys.* **9,** 3505–3522 (2009).
5. Shilling, J. E. *et al.* Measurements of the vapour pressure of cubic ice and their implications for atmospheric ice clouds. *Geophys. Res. Lett.* **33,** L17801 (2006).
6. Jensen, E. J. *et al.* Formation of large (similar or equal to 100 μm) ice crystals near the tropical tropopause. *Atmos. Chem. Phys.* **8,** 1621–1633 (2008).
7. Jensen, E. J., Pfister, L., Bui, T.-P., Lawson, P. & Baumgardner, D. Ice nucleation and cloud microphysical properties in tropical tropopause layer cirrus. *Atmos. Chem. Phys.* **10,** 1369–1384 (2010).
8. Froyd, K. D. *et al.* Aerosol composition of the tropical upper troposphere. *Atmos. Chem. Phys.* **9,** 4363–4385 (2009).
9. Murphy, D. M. *et al.* Single-particle mass spectrometry of tropospheric aerosol particles. *J. Geophys. Res. Atmos.* **111,** D23S32 (2006).
10. Murray, B. J. Inhibition of ice crystallisation in highly viscous aqueous organic acid droplets. *Atmos. Chem. Phys.* **8,** 5423–5433 (2008).
11. Zobrist, B., Marcolli, C., Pedernera, D. A. & Koop, T. Do atmospheric aerosols form glasses? *Atmos. Chem. Phys.* **8,** 5221–5244 (2008).
12. Froyd, K. D., Murphy, D. M., Lawson, P., Baumgardner, D. & Herman, R. L. Aerosols that form subvisible cirrus at the tropical tropopause. *Atmos. Chem. Phys.* **10,** 209–218 (2010).
13. Koop, T., Luo, B. P., Tsias, A. & Peter, T. Water activity as the determinant for homogeneous ice nucleation in aqueous solutions. *Nature* **406,** 611–614 (2000).
14. Möhler, O. *et al.* Experimental investigation of homogeneous freezing of sulphuric acid particles in the aerosol chamber AIDA. *Atmos. Chem. Phys.* **3,** 211–223 (2003).
15. Möhler, O. *et al.* The effect of organic coating on the heterogeneous ice nucleation efficiency of mineral dust aerosols. *Environ. Res. Lett.* **3,** 025007 (2008).
16. Koop, T. Homogeneous ice nucleation in water and aqueous solutions. *Z. Phys. Chem.* **218,** 1231–1258 (2004).
17. Cziczo, D. J. *et al.* Observations of organic species and atmospheric ice formation. *Geophys. Res. Lett.* **31,** L12116 (2004).
18. Kärcher, B. & Spichtinger, P. in *Clouds in the Perturbed Climate System, Their Relationship to Energy Balance, Atmospheric Dynamics, and Precipitation* (eds Heintzenberg, J. & Charlson, R. J.) (MIT Press, 2009).
19. Kärcher, B. Supersaturation, dehydration, and denitrification in Arctic cirrus. *Atmos. Chem. Phys.* **5,** 1757–1772 (2005).
20. Jensen, E. J. *et al.* Ice supersaturations exceeding 100% at the cold tropical tropopause: Implications for cirrus formation and dehydration. *Atmos. Chem. Phys.* **5,** 851–862 (2005).
21. Lawson, R. P. *et al.* Aircraft measurements of microphysical properties of subvisible cirrus in the tropical tropopause layer. *Atmos. Chem. Phys.* **8,** 1609–1620 (2008).
22. Gensch, I. V. *et al.* Supersaturations, microphysics and nitric acid partitioning in a cold cirrus cloud observed during CR-AVE 2006: An observation-modelling intercomparison study. *Environ. Res. Lett.* **3,** 035003 (2008).
23. Khvorostyanov, V. I., Morrison, H., Curry, J. A., Baumgardner, D. G. & Lawson, P. High supersaturation and modes of ice nucleation in thin tropopause cirrus: Simulation of the 13 July 2002 cirrus regional study of tropical anvils and cirrus layers case. *J. Geophys. Res.* **111,** D02201 (2006).
24. Spichtinger, P. & Gierens, K. M. Modelling of cirrus clouds—Part 2: Competition of different nucleation mechanisms. *Atmos. Chem. Phys.* **9,** 2319–2334 (2009).
25. Eastwood, M. L. *et al.* The effects of sulfuric acid and ammonium sulphate coatings on the ice nucleation properties of kaolinite particles. *Geophys. Res. Lett.* **36,** L02811 (2009).
26. Murray, B. J., Knopf, D. A. & Bertram, A. K. The formation of cubic ice under conditions relevant to Earth's atmosphere. *Nature* **434,** 202–205 (2005).
27. Murray, B. J. Enhanced formation of cubic ice in aqueous organic acid droplets. *Environ. Res. Lett.* **3,** 025008 (2008).
28. Murray, B. J. & Bertram, A. K. Inhibition of solute crystallisation in aqueous H^+–NH_4^+–SO_4^{2-}–H_2O droplets. *Phys. Chem. Chem. Phys.* **10,** 3287–3301 (2008).
29. Peter, T. *et al.* Ultrathin tropical tropopause clouds (UTTCs): I. Cloud morphology and occurrence. *Atmos. Chem. Phys.* **3,** 1083–1091 (2003).

30. Murphy, D. M. & Koop, T. Review of the vapour pressures of ice and supercooled water for atmospheric applications. *Q. J. R. Meteorol. Soc.* **131,** 1539–1565 (2005).

Acknowledgements

B.J.M. thanks the Natural Environment Research Council (NE/D009308/1) and the European Research Council (FP7, 240449—ICE) for fellowships. We acknowledge the FP6 European Network of Excellence Atmospheric Composition Change 'ACCENT' for travel funds (GOCE CT-2004—505337). T.W.W. thanks the Charles Brotherton Trust for a Studentship and the Aerosol Society for further financial support. We thank the AIDA operators and technicians for their support during the experiments. The water vapour measurements were partially funded by the Helmholtz Virtual Institute Aerosol Cloud Interaction (VIACI). We thank T. Leisner for helpful discussions and M. Pilling for commenting on this manuscript.

Author contributions

B.J.M. oversaw this project, sought financial support for it and wrote this manuscript. S.D. led the modelling aspects in collaboration with S.M.R.K.A. and B.K. T.W.W. analysed the data provided by the AIDA team. O.M. led the AIDA team, which included M.S., R.W., S.B., M.N. and H.S., who operated the AIDA chamber and equipment. B.J.M., T.W.W. and Z.C. helped with the AIDA experiments. V.E. and S.W. provided the analysed AIDA water vapour data.

Additional information

The authors declare no competing financial interests. Supplementary information accompanies this paper on www.nature.com/naturegeoscience. Reprints and permissions information is available online at http://npg.nature.com/reprintsandpermissions. Correspondence and requests for materials should be addressed to B.J.M.